Journal of Advanced Research in Fluid Mechanics and Thermal Sciences 94, Issue 1 (2022) 138-151

SEMARAK ILMU PUBLISHING

Journal of Advanced Research in Fluid Mechanics and Thermal Sciences

Journal homepage:
https://semarakilmu.com.my/journals/index.php/fluid_mechanics_thermal_sciences/index
ISSN: 2289-7879

Rotor Power Optimization of Horizontal Axis Wind Turbine from Variations in Airfoil Shape, Angle of Attack, and Wind Speed

Kriswanto[1,*], Fajar Romadlon[1], Dony Hidayat Al-Janan[1], Widya Aryadi[1], Rizqi Fitri Naryanto[1], Samsudin Anis[1], Imam Sukoco[1], Jamari[2]

[1] Department of Mechanical Engineering, Universitas Negeri Semarang, Gd E9 Kampus Sekaran Gunungpati, Semarang, Indonesia
[2] Department of Mechanical Engineering, University of Diponegoro, Jl. Prof. Sudharto Kampus UNDIP Tembalang, Semarang 50275, Indonesia

ARTICLE INFO

Article history:
Received 10 October 2021
Received in revised form 8 March 2022
Accepted 14 March 2022
Available online 8 April 2022

Keywords:
Airfoil; angle of attack; blade element momentum; HAWT; optimization; wind speed

ABSTRACT

This paper presents rotor power optimization of the Horizontal Axis Wind Turbine of various parameters such as airfoil, angle of attack, and wind speed. Simulation of HAWT rotor power uses Blade Element Momentum (BEM). Furthermore, optimization using the Taguchi method with $L_{16}(4^3)$ orthogonal array. The parameters used in this study were: airfoil NACA (National Advisory Committee for Aeronautics) 4412, NACA 2412, NACA 4412-NACA 2412, NACA 4412mod-NACA 2412mod; angle of attack 3˚, 4˚, 5˚, 6˚; and wind speed of 5, 6, 7, 8 (m/s). The simulation uses the general parameter at 1 MW HAWT. Several types of NACA airfoil, angle of attack, and wind speed were simulated, then optimized to obtain optimal parameters for the HAWT output power. The results of this study found the most optimal rotor power, namely the condition of the NACA 4412mod-NACA 2412mod airfoil, 3˚ angle of attack, and 8m/s wind speed. Wind speed is the most significant influence factor based on ANOVA analysis ranked 1st based on S/N ratio analysis, 2nd rank is an airfoil, and 3rd rank is the angle of attack. The higher the wind speed, the greater the rotor power generated.

1. Introduction

Numerous locations in Indonesia have the potential for wind power generation growth, with wind speeds exceeding 5m/s [1]. However, at low wind speeds of the wind power systems at the inland sites, South East Asia does not produce substantial electricity [2]. According to IEC [3], a wind speed of 5 m/s was classed as low wind speed. A rotor blade is an essential part of the advancement of wind power generation. Another component that impacts wind turbine performance is bearings, particularly ones with exceptionally low friction that influences wind turbine performance. Since there's no mechanical contact between the shaft and the rotor blade, studying Permanent Magnetic Bearings (PMB) in wind turbine prototypes to substitute mechanical bearings can enhance rotational speed and torque [4].

* *Corresponding author*
E-mail address: kriswanto@mail.unnes.ac.id

https://doi.org/10.37934/arfmts.94.1.138151

The rotor blade affects wind turbine performance, wherein it is a component that initially receives wind power before converting it to mechanical. Because of the lift and drag forces acting on the blades, wind flowing over the airfoil can cause them to rotate. A minor adjustment in dimensions can have an impact on the blade's efficiency. The High-efficiency of the wind turbines converts the kinetic energy of the wind into electric power optimised so that the blade as the initial component associated with the wind requires selecting chord, alpha (α), twist (β) values that fit, and wind speed.

Many studied have been carried out to improve the rotor shape of Horizontal Axis Wind Turbines to maximize power output. Furthermore, optimize the design of low-speed wind turbine blades by using an NRELS series airfoil with a high aerodynamic performance from the application of the Wilson design method to obtain an average power of 628318W at a wind speed of 7m/s [5]. The study implementing the BEM Method also explains the relationship between wind speed and turbine output power, that the higher the wind speed, the higher power, and then the 1.5 MW of power reached at the wind speed of 14 m/s [6]. Comparison of power, lift and drag coefficients of a wind turbine blade from aerodynamics characteristics of NACA 0012 and NACA 2412 use three simulation models and experimental results getting NACA 2412 airfoils to have higher efficiency at the Tip 7-speed ratio and have a higher maximum power output than NACA 0012. Furthermore, NACA 2412 creates more efficient turbine blades than NACA 0012 [7].

The experimental and numerical comparison of the power coefficient (Cp) and the lift-to-drag ratio of NACA 0012 airfoils with NACA 4412 airfoils revealed that the CP of the NACA 4412 is greater than the Cp of the NACA 0012 [8]. The airfoils (NACA 4412, SG6043, SD7062, and S833) were simulations of QBlade software, and the overall power coefficient (Cp) of NACA 4412 at different ends of the velocity ratio was to be superior to the other three airfoils [9]. The angle of attack is the most crucial element in determining the aerodynamics of a wind turbine revolving blade [10]. Furthermore, it has a significantly influenced performance of a wind turbine blade since it is directly proportional to the forces exerted [11]. The study of unique aerodynamic mathematical models to determine the optimal blade chord and twist angle distributions over the blade span, in which this investigation combines blade design and the airfoil analysis procedure [12].

Numerous studies on the influence of leading-edge airfoils with or without bumps aimed at the airfoil allow it to operate and perform better at higher angles of attack before stalling [13-18]. The study [13-14], [16-18] was for the airfoil on the airplane wing. Furthermore, the study of the airfoil for wind turbines with modifications to the leading edge with a bump gets the lift coefficient of the blade by adding a bump that is higher than the conventional blade [15].

According to the above literature, although research on the performance analysis of HAWT was conduct, the works are focused on certain factors, such as airfoil type, wind speed, or angle of attack. It the necessary knowledge that in HAWT performance, various factors may have distinct and simultaneous effects on the airfoil variation and angle of attack when used at low wind speeds. It emphasizes the necessity of concurrent study on optimizing airfoil type, angle of attack, and wind speed to gain better parameters of the performance of the HAWT power rotor. Therefore, the purpose of this study was to optimize the HAWT rotor power from rotor blade variations in airfoil shape, angle of attack, and low wind speed.

2. Methodology

BEM (Blade Element Momentum) method has been used in this study to obtain power output. Furthermore, the BEM method is a popular design method for the horizontal axis and vertical axis wind turbines. The main goal of the BEM model is that it is less expensive and has a shorter computing time than the CFD model [19-24]. BEM theory and CFD simulation are the most widely used approaches for predicting wind turbine performance and aerodynamic properties [25]. The mesh developed in the computational domain has a significant influence on the accuracy of CFD simulation [26] Furthermore, this approach is a model used to analyze wind turbine performance based on mechanical, geometric factors, and features [27]. The BEM is one of the design methods used to simulate and achieve the theoretical analysis of turbine rotors [28].

BEM theory base on the assumption of the forces acting on the two-dimensional blade element so that the lengthwise flow is neglected [29]. Eq. (1) and (2) is the equation of thrust and torque on a blade element theory. Figure 1-a is the local element of forces on the blade and Figure 1-b is the velocities and flow angles on the blade.

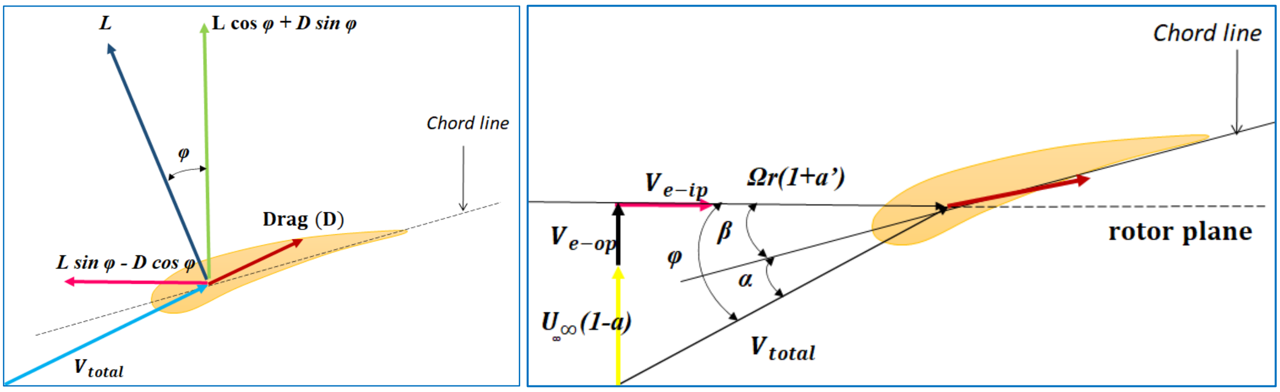

Fig. 1. Local element (a) Forces (b) Velocities and flow angles

$$dT = B\frac{1}{2}\rho V_{total}^2(C_l\cos\varphi + C_d\sin\varphi)\,cdr \tag{1}$$

$$dQ = B\frac{1}{2}\rho V_{total}^2(C_l\sin\varphi - C_d\cos\varphi)\,crdr \tag{2}$$

Where *dT* is the thrust, *dQ* is the torque on the blade sections, *B* is number of blades, *ρ* is the air density, V_{total} is the resultant velocity, C_l is the lift coefficient, C_d is the drag coefficient, *φ* the inflow angle, *c* is the airfoil chord, and r is the distance of the element from hub.

$$dT = 4\pi r\rho U_\infty^2(1-a)\,adr \tag{3}$$

$$dQ = 4\pi r^3\rho U_\infty\Omega(1-a)\,a'dr \tag{4}$$

$$a' = \frac{\omega}{2\Omega} \tag{5}$$

where *a'* is the axial induction factor, U_∞ is the velocity far downstream, ω is the blade rotation speed, and Ω is the angular speed.

This study focuses on optimizing the power rotor of HAWT (Horizontal Axis Wind Turbine) from the factors of airfoils, angle of attack, and wind speeds. Table 1 shows the specification of HAWT which is simulated using the BEM method.

It is important to predict the power rotor at low wind speeds according to wind conditions in Southeast Asia. As seen in Eq. (6), wind power is proportional to the cube of wind speed.

$$P = {}^1\!/_2\,\rho A w^3 \tag{6}$$

where *w* is the wind speed and *A* is the cross-sectional area of blade.

Table 1
Parameter setup of the 1 MW HAWT Model

Specification	Value
Air density (kg/m^3)	1.225
Number of blades	3
Blade length (m)	55
Radius of hub (m)	1.25
Tower height (m)	110
Swept area (m^2)	10,023.67

The optimization method used is the Taguchi method, a methodology in engineering that aims to improve the quality of products and processes, moreover reduce costs and resources to a minimum [30-32]. The target of the Taguchi method is to make the product robust against noise so commonly referred to as Robust Design [23-39].

A two-way analysis of variance used for the data has two or more factors over two or more levels. The analysis table consists of the degrees of freedom calculation, the number of squares, the average number of squares, and the F-ratio. The S/N ratio is used to find the factors that influence the power variance. The characteristics S/N ratio used is larger the better that calculated by Eq. (7).

$$S/N_L = -10\ log\left(\frac{1}{n}\sum_{i=1}^{n}\frac{1}{y^2}\right) \tag{7}$$

The chosen orthogonal matrix is a matrix that has a degree of freedom value equal to or greater than the experimental degree of freedom value. The degrees of freedom for the matrix $L_{16}(4^3)$. Degrees of freedom $L_{16}(4^3)$ = (many factors) x (many levels = -1) = 3 x (4-1) = 9. So, the chosen orthogonal matrix is matrix $L_{16}(4^3)$. Table 2 is the parameter used in the rotor power optimization. Then Table 3 shows the orthogonal matrix $L_{16}(4^3)$, which has three factors and four levels. Three factors are airfoil, angle of attack, and wind speed. Wind speeds range from 5-8 m/s were classified as low wind speeds according to IEC 61400-1 (International Electrotechnical Commission) [24].

Table 2
Independent Variable and Level Setting

Factor	1	2	3	4
Airfoil (NACA)	4412	2412	4412-2412	4412mod-2412mod
Angle of attack (˚)	3	4	5	6
Wind speed (m/s)	5	6	7	8

Table 3
The Orthogonal Matrix L_{16} (4^3)

No.	Factor Control Airfoil (NACA)	Angle of Attack, α (°)	Wind Speed, v (m/s)
1	4412	3	5
2	4412	4	6
3	4412	5	7
4	4412	6	8
5	2412	3	6
6	2412	4	5
7	2412	5	8
8	2412	6	7
9	4412-2412	3	7
10	4412-2412	4	8
11	4412-2412	5	5
12	4412-2412	6	6
13	4412mod-2412mod	3	8
14	4412mod-2412mod	4	7
15	4412mod-2412mod	5	6
16	4412mod-2412mod	6	5

There are two types of main airfoils in this study, namely NACA 4412 (Figure 2) as the 1st variation and NACA 2412 (Figure 3) for the 2nd variation. Furthermore, the 3rd variation uses a combination of NACA 4412 with NACA 2412, then and the last variation is a modification of the lower surface prior to the trailing edge of the two airfoils NACA4412mod-2412mod.

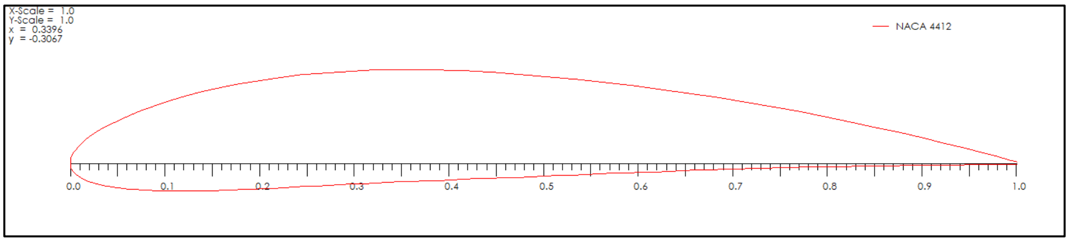

Fig. 2. Airfoil NACA 4412

The form difference of the NACA 4412 and NACA 2412 airfoils before-after modification is found on the lower surface before the trailing edge such as the area marked in circular red (modified form) in Figures 4 and Figure 5. The standard NACA airfoil with NACA modification has a y-coordinate difference of 0.06 for the NACA 4412 airfoil (Figure 6) and 0.0148 for the 2412 airfoil (Figure 7) on the lower surface at points 0.9 to 1.

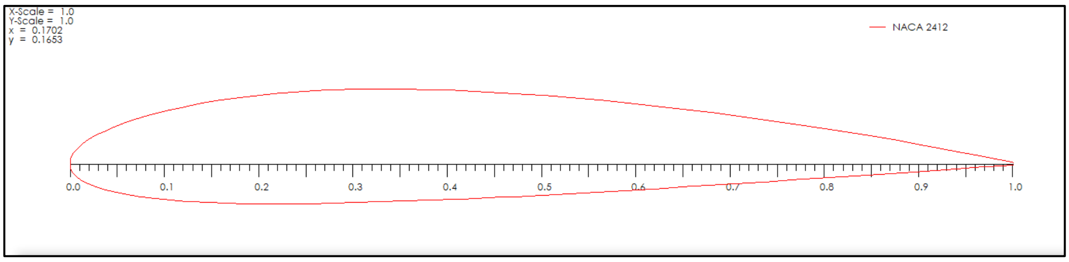

Fig. 3. Airfoil NACA 2412

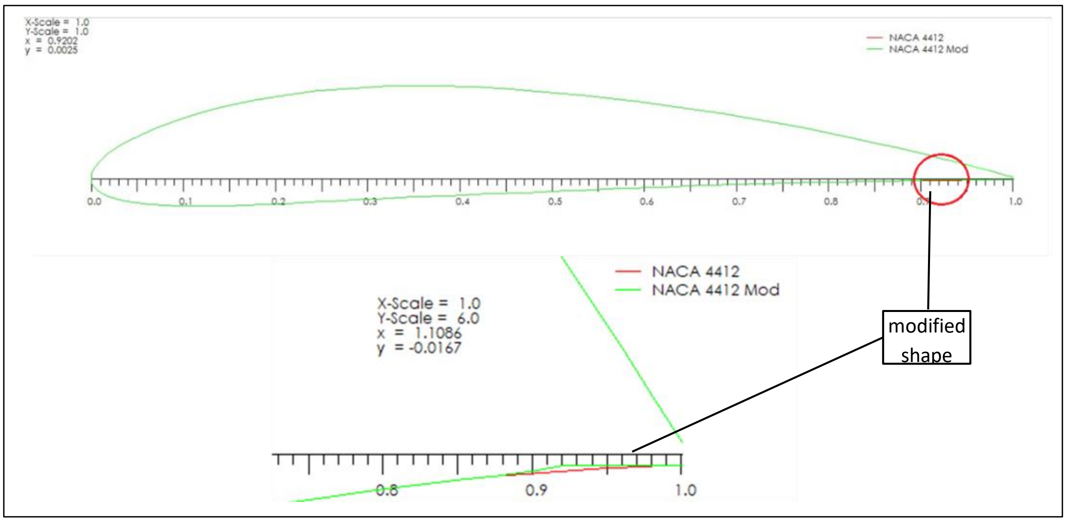

Fig. 4. NACA 4412mod

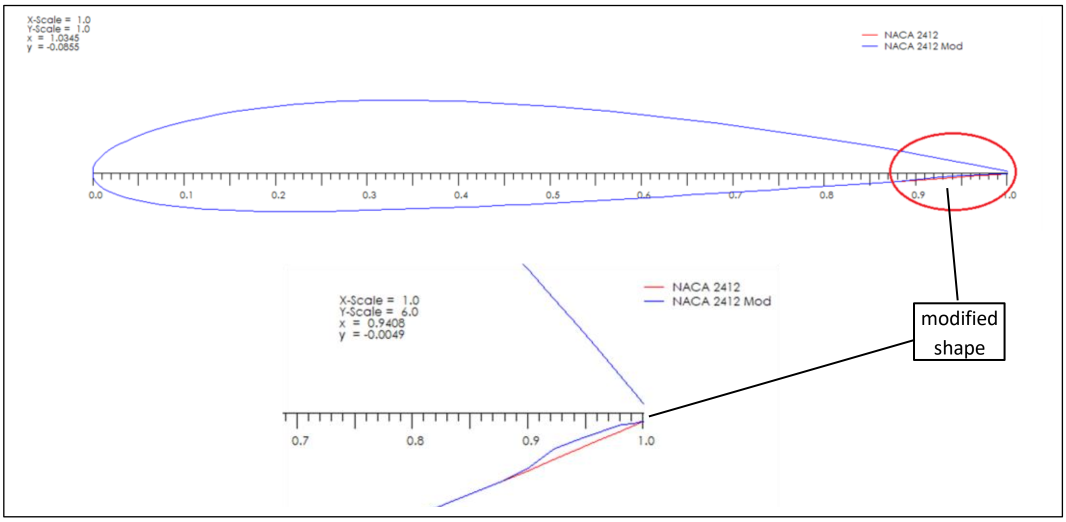

Fig. 5. NACA 2412mod

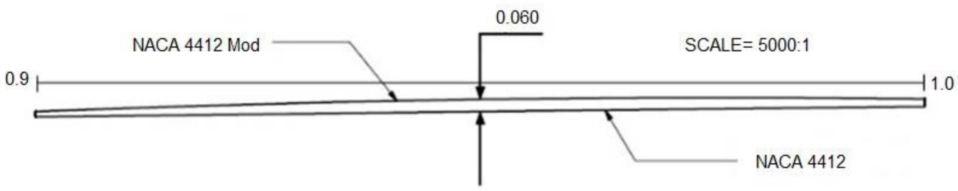

Fig. 6. Differences between Standard Airfoil and Modified NACA 4412

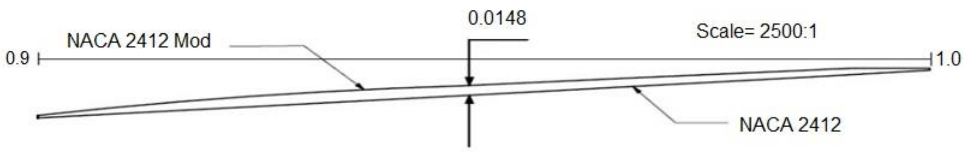

Fig. 7. Differences between Standard Airfoil and Modified NACA 2412

Figure 8 shows the angle of attack on the airfoil and the variations of the angle of attack presented in Table 1. The angle of attack should not be too large caused the air will no longer follow on the airfoil surface. Therefore, airflow will separate above the airfoil, and vortex will occur behind the airfoil leading edge. Consequently, the drag force increases significantly, and the lifting force decreases. This situation is called a stall, and the critical angle at which the transition occurs is called the stall angle of attack.

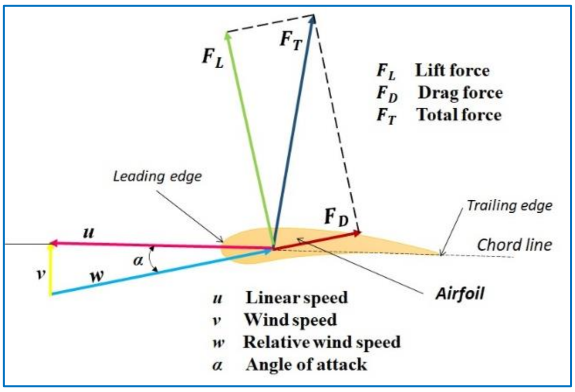

Fig. 8. Angle of attack and relative wind speed

The lift coefficient is very influential on the performance of a turbine. The value of the lift coefficient will change with the change in the value of the angle of attack. Variations of it on the airfoil, the value of C_L will increase as the angle of attack is adjusted until C_L reaches its maximum value. The C_L calculation use Eq. (8).

$$C_L = \frac{F_L}{{}^1/_2 \rho w^2 A} \tag{8}$$

Where C_L is the lift coefficient and F_L is lift force.

3. Results

The validation has been done by comparing the power output between the CFD method by Oukassou [7] with the BEM method used in the present study. The power rotor has been simulated with the same parameters as the CFD (see Table 4). Hereafter, the power output generated by the BEM method is shown in Figure 9. The difference of CFD-BEM values is not so far apart, which is 0.4%. Therefore, the BEM method was appropriate to use to simulate rotor power accord the boundary conditions. Validation between the two models, namely CFD and BEM Theory, is carried out to verify the results of the turbin performance values are reasonable [40].

Table 4
Validation of BEM method in the present study with CFD methods [7]

Method	Airfoil	v (m/s)	Numbers of Blade	TSR	ρ (kg/m^3)	N (rpm)	P(kW)
CFD	NACA 0012	12	3	7	1,225	12.10	5
BEM	NACA 0012	12	3	7	1,225	12.10	4,98
% variation							0,4

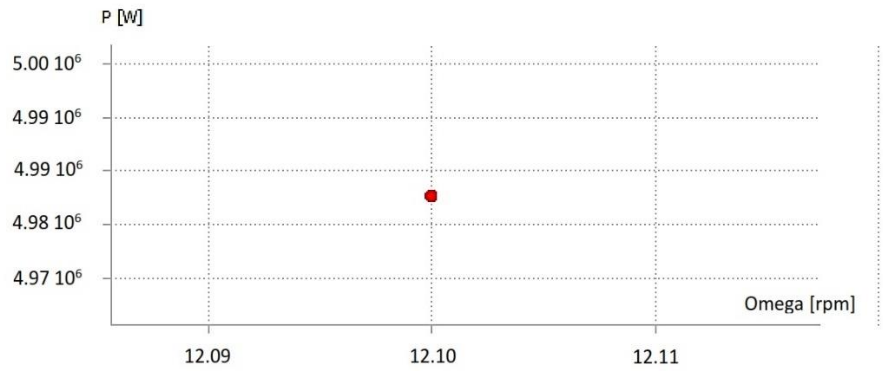

Fig. 9. Graph of power output using the BEM Method

where v is wind speed, *TSR* is a tip speed ratio, N is rotor rotational speed, and P is the power output of the HAWT. Each rotor blade design consists of 10 segments, wherein segments 1 and 2 use circular foil. Furthermore, the third to the last segment uses either the NACA 2412 or NACA 4412 airfoil design, a combination of both, and the modified combination of the two airfoils. The design and geometry of the blade design as shown in Figure 10 to 13, which are the angle of attack 3˚.

The results of the turbine rotor power simulation using the BEM method on the Qblade software are adjusted to the predetermined parameters. The power data the simulation results are shown in Table 5.

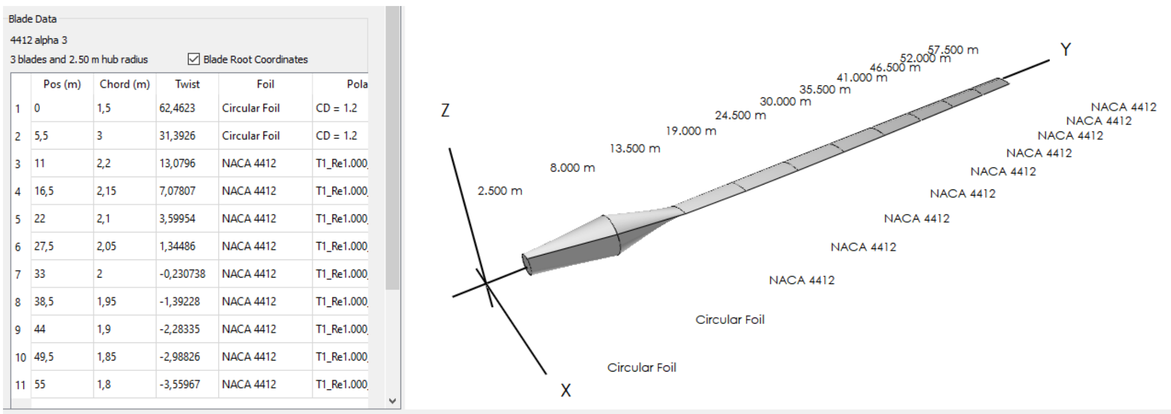

	Pos (m)	Chord (m)	Twist	Foil	Pola
1	0	1,5	62,4623	Circular Foil	CD = 1.2
2	5,5	3	31,3926	Circular Foil	CD = 1.2
3	11	2,2	13,0796	NACA 4412	T1_Re1.000
4	16,5	2,15	7,07807	NACA 4412	T1_Re1.000
5	22	2,1	3,59954	NACA 4412	T1_Re1.000
6	27,5	2,05	1,34486	NACA 4412	T1_Re1.000
7	33	2	-0,230738	NACA 4412	T1_Re1.000
8	38,5	1,95	-1,39228	NACA 4412	T1_Re1.000
9	44	1,9	-2,28335	NACA 4412	T1_Re1.000
10	49,5	1,85	-2,98826	NACA 4412	T1_Re1.000
11	55	1,8	-3,55967	NACA 4412	T1_Re1.000

Fig. 10. Rotor blade design use NACA 412 airfoil

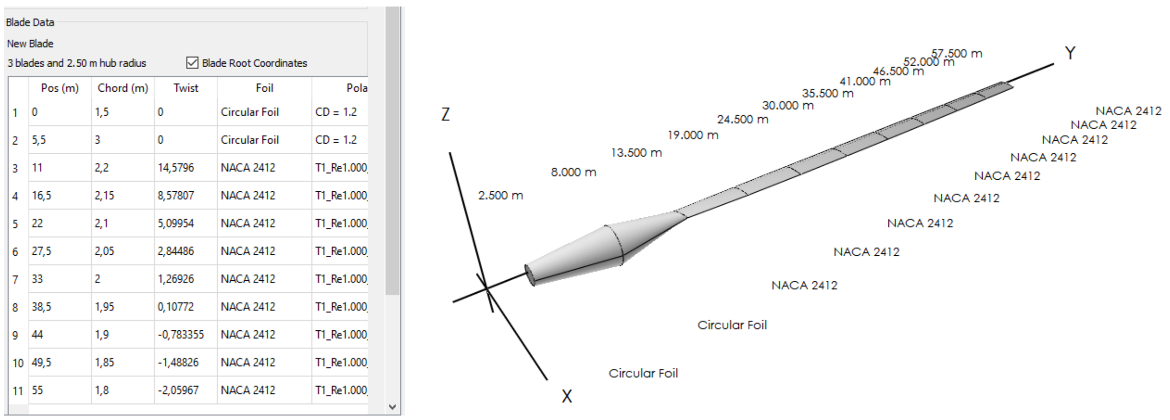

	Pos (m)	Chord (m)	Twist	Foil	Pola
1	0	1,5	0	Circular Foil	CD = 1.2
2	5,5	3	0	Circular Foil	CD = 1.2
3	11	2,2	14,5796	NACA 2412	T1_Re1.000
4	16,5	2,15	8,57807	NACA 2412	T1_Re1.000
5	22	2,1	5,09954	NACA 2412	T1_Re1.000
6	27,5	2,05	2,84486	NACA 2412	T1_Re1.000
7	33	2	1,26926	NACA 2412	T1_Re1.000
8	38,5	1,95	0,10772	NACA 2412	T1_Re1.000
9	44	1,9	-0,783355	NACA 2412	T1_Re1.000
10	49,5	1,85	-1,48826	NACA 2412	T1_Re1.000
11	55	1,8	-2,05967	NACA 2412	T1_Re1.000

Fig. 11. Rotor blade design use NACA 2412 airfoil

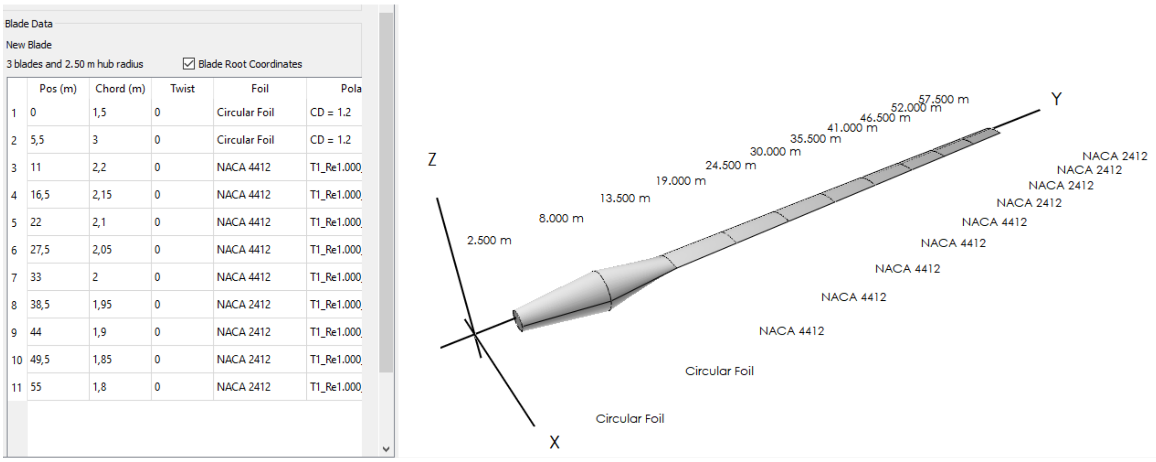

Fig. 12. Rotor blade design uses a combination of NACA 4412 with NACA 2412

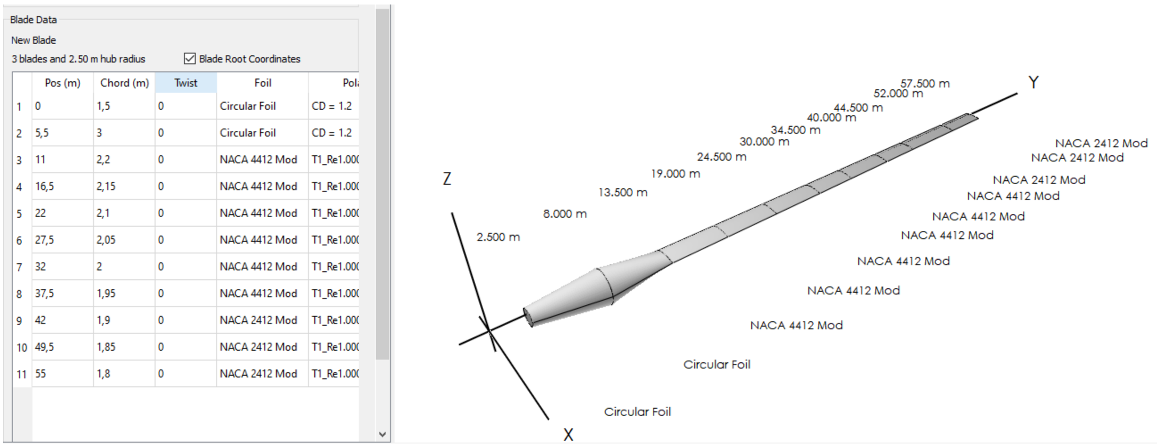

Fig. 13. Rotor blade design uses modified airfoil NACA 4412 and NACA 2412

Table 5
HAWT Power rotor of L_{16} (4^3)

No.	Factor Control Airfoil (NACA)	Angle of Attack, α (˚)	Wind Speed, v (m/s)	Power (kW)
1.	4412	3	5	366
2.	4412	4	6	626
3.	4412	5	7	975
4.	4412	6	8	1420
5.	2412	3	6	619
6.	2412	4	5	358
7.	2412	5	8	1482
8.	2412	6	7	992
9.	4412-2412	3	7	1045
10.	4412-2412	4	8	1546
11.	4412-2412	5	5	372
12.	4412-2412	6	6	634
13.	4412mod-2412mod	3	8	1564
14.	4412mod-2412mod	4	7	1037
15.	4412mod-2412mod	5	6	646
16.	4412mod-2412mod	6	5	368

ANOVA is used to determine the effect of each factor (airfoil, angle of attack, and wind speed) on the turbine rotor power produced. Table 6 is the analysis of the variance of each factor at each level tested for the rotor power. The analysis (see table 6) shows that the airfoil and wind speed factors significantly affect the turbine rotor power because the analysis value is less than the specified P value (0.05). The largest F value (2,424.3) is found in the wind speed factor so that it is the most influential factor on turbine rotor power compared to airfoil and angle of attack. The table below shows the F and P values for the contribution test of the parameters. Wind speed is the most significant influencing factor in generating power conforms the power output is proportional to the cube of wind speed, according to Eq. (6). As the wind speed increases, so does the power extracted by the turbine increased [6].

Table 6
Analysis of Variance on Power Rotor

Source	DF	Seq SS	Adj SS	Adj MS	F	P
Airfoil	3	9,295	9,295	3.098	7.7	0.02
Angle of Attack	3	5.180	5.180	1,727	4.29	0.06
Wind Speed	3	2,926,710	2,926,710	975.570	2,424.3	0
Error	6	2.415	2.415	402		
Total	15	2,943,600				

S = 20.06 R-Sq = 99.92% R-Sq (Adj) = 99.97%

Calculation of the S/N ratio of roundness through a combination of levels of each factor uses Eq. (2). The result of S/N ratio as shown in Table 7.

Table 7 shows the S/N ratio value of rotor power for each factor. The S/N ratio gets the wind speed factor was ranked 1st or the most significant effect to the power rotor. The data of the S/N ratio was plotted in Figure 13, which shows of each factor affects each level. The airfoil factor at level 4 has a greater influence on the airfoil NACA 4412mod-NACA 2412mod provides a better output of rotor power. Furthermore, to the angle of attack factor, it is known that level 1 has a significant influence over the others (2, 3, and 4). The angle of attack of 3˚ gives a better rotor power output. On another factor, Level 4 of wind speed has a higher effect than levels 1, 2, and 3.

Table 7
Response of S/N Ratio of Roundness of Effect of Factor

Level	Airfoil	Angle of Attack	Wind Speed
1	57.51	57.84	51.27
2	57.56	57.78	56.00
3	57.90	57.70	60,10
4	57.93	57.58	63.53
delta	0.42	0.26	12.26
rank	2	3	1

The speed factor has an S/N ratio of 12.26 so this factor has a significant effect on the value of generating rotor power. Based on the plot (Figure 14), the significant influence on the power rotor is the airfoil parameter NACA 4412mod-NACA 2412mod, 3˚an angle of attack, and 8m/s of wind speed. Accordingly, these parameters are the optimum value of the power rotor.

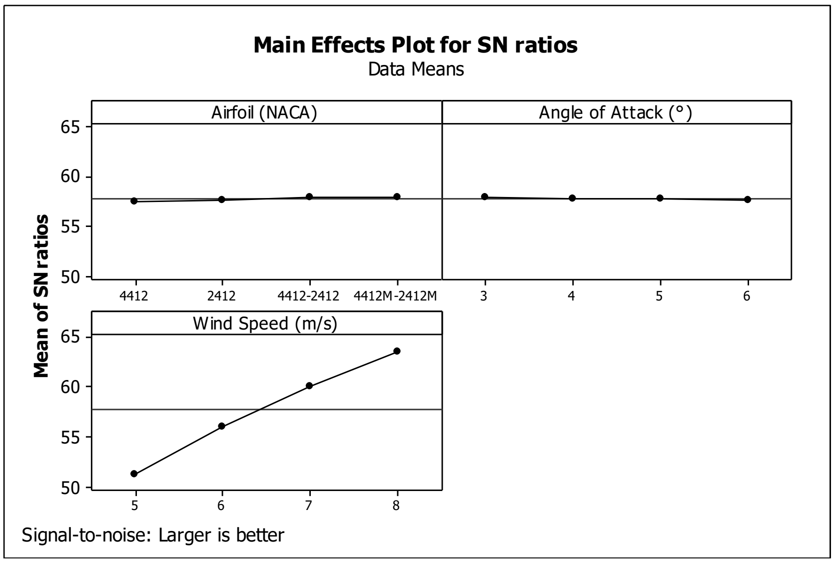

Fig. 14. S/N Ratio Plot Rotor Power

The optimum power was obtained on the NACA airfoil modified. This is because the lift coefficient of the modified NACA airfoil (4412mod-2412mod) is greater than the standard NACA (4412-2412) with the CL value increased by 0.002. These results were obtained from the BEM method simulation as shown in Figure 15. Even though the lift coefficient insignificant increase, but its contributed to an increase in the performance of HAWT.

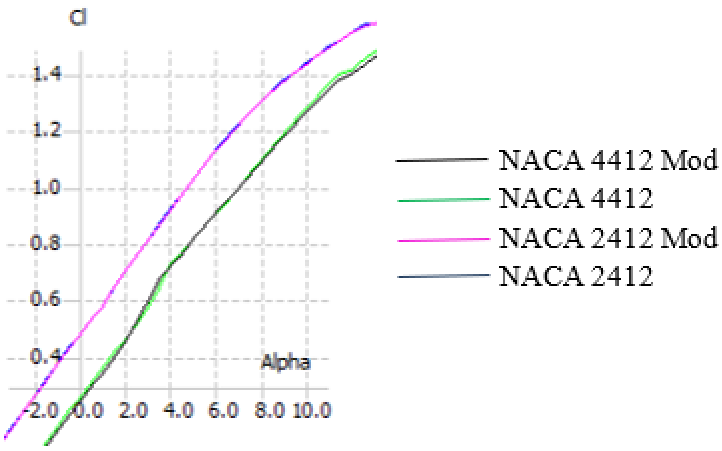

Fig. 15. The plot of lift coefficient versus angle of attack of Airfoil in the study

Based on the simulation result (Figure 15), the coefficient of lift of each airfoil increased as the angle of attack increases. Seen at angle of attach of 10˚, the C_L value of at least 1.2 is higher than the C_L limit in this study of 6 ˚, with a minimum CL of 0.6. Due to the obvious unstable character of the flow at high angles of attack, there is a considerable degree of uncertainty in the performance of airfoils and, as a result, in the performance of blades [41]. The angle of attack in this study was 3-6 ˚ further the findings of S/N ratio computation show that the higher the alpha, the lower the value of the S/N ratio. The difference in the decrease of the S/N ratio of 0.26 is too small on the increase in the alpha value, then concluded that the angle of attack factor has no significant effect on the rotor power.

4. Conclusions

HAWT rotor blades on several variations of airfoils, angles of attack, and wind speed according to L16(4^3) orthogonal array were simulated to generate output power. The rotor power optimum (1.56MW) obtain on the NACA 4412mod-2412mod airfoils parameters with the angle of attack of 3˚ and wind speed of 8 m/s. Wind speed is the most significant influencing factor based on ANOVA analysis, then was 1st ranked based on S/N ratio analysis. Furthermore, the 2nd rank that influences consecutively is an airfoil, and the last rank is the angle of attack. The higher the wind speed, the greater the rotor power generated. The aerodynamic characteristics of airfoil NACA 4412 and NACA 2412 after being modified on the lower surface near the trailing edge have been simulated with the BEM method produce lift coefficient greater than NACA 4412 and NACA 2412 before modification. The lift coefficient of the NACA 4412 and NACA 2412 after modified was rose by 0.002 for both airfoils types that contribute positively to increasing the power performance of the HAWT rotor.

References

[1] Sutijastoto, F.X. 2020. Book of Strategic Plan of the Directorate General of New, Renewable Energy and Energy Conservation for 2020-2024. Ministry of Energy and Mineral Resources

[2] Gitano-Briggs, Horizon. "Low speed wind turbine design." *Advances in Wind Power* (2012).

[3] Katsigiannis, Yiannis A., George S. Stavrakakis, and Christodoulos Pharconides. "Effect of wind turbine classes on the electricity production of wind farms in Cyprus Island." In *Conference Papers in Science*, vol. 2013. Hindawi, 2013. https://doi.org/10.1155/2013/750958

[4] Kriswanto, and Jamari. "Radial forces analysis and rotational speed test of radial permanent magnetic bearing for horizontal axis wind turbine applications." In *AIP Conference Proceedings*, vol. 1725, no. 1, p. 020034. AIP Publishing LLC, 2016. https://doi.org/10.1063/1.4945488

[5] Yunhao, Chen, Hu Danmei, and Zhao Zhenjiang. "Low-speed wind turbine design based on Wilson theory." In *IOP Conference Series: Earth and Environmental Science*, vol. 621, no. 1, p. 012175. IOP Publishing, 2021. https://doi.org/10.1088/1755-1315/621/1/012175

[6] Ibrahim, A. M., S. F. Abdullah, and M. B. Salih. "Modeling and simulation of 1.5 MW wind turbine." *Int. Journal of Applied Engineering* 13, no. 10 (2018): 7882-7888.

[7] Oukassou, Karim, Sanaa El Mouhsine, Abdellah El Hajjaji, and Bousselham Kharbouch. "Comparison of the power, lift and drag coefficients of wind turbine blade from aerodynamics characteristics of Naca0012 and Naca2412." *Procedia Manufacturing* 32 (2019): 983-990. https://doi.org/10.1016/j.promfg.2019.02.312

[8] Rocha, PA Costa, HH Barbosa Rocha, FO Moura Carneiro, ME Vieira da Silva, and C. Freitas de Andrade. "A case study on the calibration of the k–ω SST (shear stress transport) turbulence model for small scale wind turbines designed with cambered and symmetrical airfoils." *Energy* 97 (2016): 144-150. https://doi.org/10.1016/j.energy.2015.12.081

[9] Said, Ali, Mazharul Islam, A. K. M. Mohiuddin, and Moumen Idres. "Performance analysis of a small capacity horizontal axis wind turbine using QBlade." *International Journal of Recent Technology and Engineering* 7, no. 6 (2019): 153-157.

[10] Zhong, Wei, Wen Zhong Shen, Tong Guang Wang, and Wei Jun Zhu. "A new method of determination of the angle of attack on rotating wind turbine blades." *Energies* 12, no. 20 (2019): 4012. https://doi.org/10.3390/en12204012

[11] Gallant, T. E., and D. A. Johnson. "In-blade angle of attack measurement and comparison with models." In *Journal of Physics: Conference Series*, vol. 753, no. 7, p. 072007. IOP Publishing, 2016. https://doi.org/10.1088/1742-6596/753/7/072007

[12] Tang, Xinzi, Xuanqing Huang, Ruitao Peng, and Xiongwei Liu. "A direct approach of design optimization for small horizontal axis wind turbine blades." *Procedia CIRP* 36 (2015): 12-16. https://doi.org/10.1016/j.procir.2015.01.047

[13] Zhao, Ming, Mingming Zhang, and Jianzhong Xu. "Numerical simulation of flow characteristics behind the aerodynamic performances on an airfoil with leading edge protuberances." *Engineering Applications of Computational Fluid Mechanics*11, no. 1 (2017): 193-209.

[14] Kunya, Bashir Isyaku, Clement O. Folayan, Gyang Yakubu Pam, Fatai Olukayode Anafi, and Nura Muaz Muhammad. "Experimental and Numerical Study of the Effect of Varying Sinusoidal Bumps Height at the Leading

Edge of the NASA LS (1)-0413 Airfoil at Low Reynolds Number." *CFD Letters* 11, no. 3 (2019): 129-144.
[15] Kunya, Bashir Isyaku, Clement Olaloye Folayan, Gyang Yakubu Pam, Fatai Olukayode Anafi, and Nura Mu'az Muhammad. "Performance study of Whale-Inspired Wind Turbine Blade at Low Wind Speed Using Numerical Method." *CFD Letters* 11, no. 7 (2019): 11-25.
[16] Ali, Jaffar Syed Mohamed, and M. Mubin Saleh. "Experimental and numerical study on the aerodynamics and stability characteristics of a canard aircraft." *Journal of Advanced Research in Fluid Mechanics and Thermal Sciences* 53, no. 2 (2019): 165-174.
[17] Hakim, Muhammad Syahmi Abdul, Mastura Ab Wahid, Norazila Othman, Shabudin Mat, Shuhaimi Mansor, Md Nizam Dahalan, and Wan Khairuddin Wan Ali. "The effects of Reynolds number on flow separation of Naca Aerofoil." *Journal of Advanced Research in Fluid Mechanics and Thermal Sciences* 47, no. 1 (2018): 56-68.
[18] Tajuddin, Nurulhuda, Shabudin Mat, Mazuriah Said, and Shumaimi Mansor. "Flow characteristic of blunt-edged delta wing at high angle of attack." *Journal of Advanced Research in Fluid Mechanics and Thermal Sciences* 39, no. 1 (2017): 17-25.
[19] Velázquez, Miguel Toledo, Marcelino Vega Del Carmen, Juan Abugaber Francis, Luis A. Moreno Pacheco, and Guilibaldo Tolentino Eslava. "Design and experimentation of a 1 MW horizontal axis wind turbine." *Journal of Power and Energy Engineering* 2014 (2014).https://doi.org/10.4236/jpee.2014.21002
[20] Marten, David, Jan Wendler, Georgios Pechlivanoglou, Christian Navid Nayeri, and Christian Oliver Paschereit. "QBLADE: an open source tool for design and simulation of horizontal and vertical axis wind turbines." *International Journal of Emerging Technology and Advanced Engineering* 3, no. 3 (2013): 264-269.
[21] Koç, Emre, Onur Gunel, and Tahir Yavuz. "Mini-Scaled Horizontal Axis Wind Turbine Analysis by QBlade and CFD." *International Journal of Energy Applications and Technologies*3, no. 2 (2016): 87-92.
[22] Marten, David, Matthew Lennie, Georgios Pechlivanoglou, Christian Navid Nayeri, and Christian Oliver Paschereit. "Implementation, optimization and validation of a nonlinear lifting line free vortex wake module within the wind turbine simulation code QBlade." In *Turbo Expo: Power for Land, Sea, and Air*, vol. 56802, p. V009T46A019. American Society of Mechanical Engineers, 2015. https://doi.org/10.1115/1.4031872
[23] Wendler, Juliane, David Marten, George Pechlivanoglou, Christian Navid Nayeri, and Christian Oliver Paschereit. "An unsteady aerodynamics model for lifting line free vortex wake simulations of hawt and vawt in qblade." In *Turbo Expo: Power for Land, Sea, and Air*, vol. 49873, p. V009T46A011. American Society of Mechanical Engineers, 2016. https://doi.org/10.1115/GT2016-57184
[24] Husaru, D. E., P. D. Bârsănescu, and D. Zahariea. "Effect of yaw angle on the global performances of Horizontal Axis Wind Turbine-QBlade simulation." In *IOP Conference Series: Materials Science and Engineering*, vol. 595, no. 1, p. 012047. IOP Publishing, 2019. https://doi.org/10.1088/1757-899X/595/1/012047
[25] Koç, Emre, Onur Günel, and Tahir Yavuz. "Comparison of Qblade and CFD results for small-scaled horizontal axis wind turbine analysis." In *2016 IEEE International Conference on Renewable Energy Research and Applications (ICRERA)*, pp. 204-209. IEEE, 2016. https://doi.org/10.1109/ICRERA.2016.7884538
[26] Zakaria, Ahmad, and Mohd Shahrul Nizam Ibrahim. "Velocity Pattern Analysis of Multiple Savonius Wind Turbines Arrays." (2021). https://doi.org/10.37934/cfdl.12.3.3138
[27] Ledoux J, Riffo S, and Salomon J. 2020. *Analysis of the Blade Element Momentum Theory*. 2020. ⟨hal-02550763⟩.
[28] Alaskari, Mustafa, Oday Abdullah, and Mahir H. Majeed. "Analysis of wind turbine using QBlade software." In *IOP conference series: materials science and engineering*, vol. 518, no. 3, p. 032020. IOP Publishing, 2019. https://doi.org/10.1088/1757-899X/518/3/032020
[29] Moriarty, J., and A. Hansen. *AeroDyn Theory Manual, NREL Tecnical Report*. NREL/TP-500-36881, 2005. https://doi.org/10.2172/15014831
[30] Shamsuddin, Shahidah Arina, Mohd Nazree Derman, Uda Hashim, Muhammad Kashif, Tijjani Adam, Nur Hamidah Abdul Halim, and Muhammad Faheem Mohd Tahir. "Nitric acid treated multi-walled carbon nanotubes optimized by Taguchi method." In *AIP Conference Proceedings*, vol. 1756, no. 1, p. 090002. AIP Publishing LLC, 2016. https://doi.org/10.1063/1.4958783
[31] Hanizam, Hashim, Mohd Shukor Salleh, Mohd Zaidi Omar, and Abu Bakar Sulong. "Optimisation of mechanical stir casting parameters for fabrication of carbon nanotubes–aluminium alloy composite through Taguchi method." *Journal of Materials Research and Technology* 8, no. 2 (2019): 2223-2231. https://doi.org/10.1016/j.jmrt.2019.02.008
[32] Babayigit, Bilal, and Ercan Senyigit. "Design optimization of circular antenna arrays using Taguchi method." *Neural Computing and Applications* 28, no. 6 (2017): 1443-1452. https://doi.org/10.1007/s00521-015-2162-y
[33] Shi, Zhou, Xiaodong Sun, Yingfeng Cai, and Zebin Yang. "Robust design optimization of a five-phase PM hub motor for fault-tolerant operation based on Taguchi method." *IEEE Transactions on Energy Conversion* 35, no. 4 (2020): 2036-2044. https://doi.org/10.1109/TEC.2020.2989438
[34] Ebro, Martin, and Thomas J. Howard. "Robust design principles for reducing variation in functional

performance." *Journal of Engineering Design* 27, no. 1-3 (2016): 75-92. https://doi.org/10.1080/09544828.2015.1103844
[35] Barea, Rafael, Simón Novoa, Francisco Herrera, Beatriz Achiaga, and Nuria Candela. "A geometrical robust design using the Taguchi method: application to a fatigue analysis of a right angle bracket." *Dyna* 85, no. 205 (2018): 37-46. https://doi.org/10.15446/dyna.v85n205.67547
[36] Diao, Kaikai, Xiaodong Sun, Gang Lei, Gerd Bramerdorfer, Youguang Guo, and Jianguo Zhu. "System-level robust design optimization of a switched reluctance motor drive system considering multiple driving cycles." *IEEE Transactions on Energy Conversion* 36, no. 1 (2020): 348-357. https://doi.org/10.1109/TEC.2020.3009408
[37] Lei, Gang, Chengcheng Liu, Yanbin Li, Dezhi Chen, Youguang Guo, and Jianguo Zhu. "Robust design optimization of a high-temperature superconducting linear synchronous motor based on Taguchi method." *IEEE Transactions on Applied Superconductivity* 29, no. 2 (2018): 1-6. https://doi.org/10.1109/TASC.2018.2882426
[38] Abhiram, D. R., Ranjan Ganguli, Dineshkumar Harursampath, and Peretz P. Friedmann. "Robust design of small unmanned helicopter for hover performance using Taguchi method." *Journal of Aircraft* 55, no. 4 (2018): 1746-1753. https://doi.org/10.2514/1.C034539
[39] Hu, Yi, and Singiresu S. Rao. "Robust design of horizontal axis wind turbines using Taguchi method." *Journal of Mechanical Design* 133, no. 11 (2011). https://doi.org/10.1115/1.4004989
[40] Takey, Mohamed, Tholudin Mat Lazim, Iskandar Shah Ishak, NAR Nik Mohd, and Norazila Othman. "Computational Investigation of a Wind Turbine Shrouded with a Circular Ring." *CFD Letters* 12, no. 10 (2020): 40-51. https://doi.org/10.37934/cfdl.12.10.4051
[41] Timmer, W. A., and C. Bak. "Aerodynamic characteristics of wind turbine blade airfoils." In *Advances in wind turbine blade design and materials*, pp. 109-149. Woodhead Publishing, 2013. https://doi.org/10.1533/9780857097286.1.109